Compact Modeling of BJT Self-heating in Circuit Simulation

David T. Zweidinger, Sang-Gug Lee, and Robert M. Fox
339 Larsen Hall, Dept. of Electrical Engineering, University of Florida, Gainesville, FL 32611

Abstract

A hierarchy of models for BJT self-heating has been implemented in SPICE DC and AC analyses. The modifications can greatly improve accuracy, especially with analog circuits. Details of the software modifications are presented, along with simulation results.

1 Introduction

As current densities and thermal spreading impedances rise with bipolar transistor scaling, collector-to-emitter thermal feedback causes increasingly significant errors in circuit simulation. For example, in a device with thermal spreading impedance of 200 °C/W and Early Voltage V_A = 150 V, the output resistance drops below one-half that predicted by the Gummel-Poon model for all currents greater than 500 μA [1]. This localized heating is in contrast to chip and package heating effects, which are extrinsic to the operation of the device. Previous efforts at including thermal effects in circuit simulation have been numerically intensive [2], have been based on inefficient and inconvenient subcircuit approaches [3], or have been based on simplified, empirical thermal models [4]. This paper describes the first instance in which predictive compact models for local heating have been installed in SPICE DC and AC analyses. The enhanced modeling greatly improves accuracy but is largely transparent to the user.

TH0424 - 2/92/0000-0219 $1.00 © 1992 IEEE

2 Thermal Spreading Impedance Model

The thermal impedance model, valid for rectangular emitters with junction isolation, has been described previously [5]. An outline of the derivation follows. The thermal impedance for the temperature rise at a point in a uniform medium due to a sinusoidal heat source a distance r away is

$$Z_{TH}(r,s) = \frac{1}{4\pi K r} exp\left(-r\sqrt{\frac{s}{\kappa}}\right) \tag{1}$$

where K is the thermal conductivity, κ is the thermal diffusivity, and s is the complex frequency. For s = 0, this equation gives the thermal resistance R_{TH} for the point source. An image point source is added to model an adiabatic plane between the two sources. R_{TH} is integrated over the collector space-charge region (SCR) and its image to predict BJT thermal resistance at any point in the semiconductor. Least-squares polynomial fits are used to approximate the integral.

The BJT common-emitter y-parameters are corrected to include thermal feedback using [6]

$$Y_{mn} = \frac{Y_{mne} + T_{CF}(I_m) Z_{TH} I_m I_n}{1 - T_{CF}(I_m) Z_{TH} P} \tag{2}$$

where m or n = 1 for the base or 2 for the collector, Y_{mne} is the uncorrected electrical y-parameter, P is the dissipated power, and $T_{CF}(I_m)$ is the fractional temperature coefficient of the base or collector current.

In the SPICE BJT model implementation, three levels of modeling are available to describe the thermal impedance. The first level is fully empirical: the user supplies thermal resistance R_{TH} and thermal capacitance C_{TH}, which are used for the real and imaginary parts of the thermal impedance for all frequencies. The second level is partially physics-based: the user supplies a value for R_{TH}, which is used to generate an effective emitter-to-collector distance r, which is used in (1) to compute Z_{TH}. This model generally provides more accurate frequency response than the single-pole, all-empirical approach. The final level is fully predictive and scalable: the user supplies emitter width and length, collector-base junction depth, and epi-layer doping (N_{EPI}). These are used with the above-mentioned polynomials to compute r in (1), which is used to find Z_{TH}. Non-zero values of input parameters N_{EPI}, R_{TH}, and C_{TH} set flags which control the level of modeling.

3 DC Analysis

To include thermal effects, the SPICE DC analysis required modification in three areas. First, the large-signal currents and all temperature-dependent parameters were adjusted to reflect the local temperature. Second, the admittance matrix was modified to include thermal effects using (2). Finally, the convergence criteria were modified to ensure convergence of the local temperature.

To compute the local temperature for each Newton-Raphson iteration, the terminal currents and voltages from the previous iteration are first retrieved from the state vector. The local temperature is then computed using $T = P \bullet R_{TH} + T_0$, where T_0 is the nominal temperature. To avoid non-convergence due to thermal runaway, the temperature is limited to a user-defined maximum. Using the new local temperature, all temperature-dependent quantities are updated using the standard SPICE temperature dependencies, and the new terminal currents and their derivatives are computed. The fractional temperature coefficients of the currents are also computed, using

$$T_{CF}(I_C) = T_{CF}(I_{be1})\left[1 - \frac{I_C}{IKF}2K_{q1}NK\left(1+4\frac{I_{be1}}{IKF}\right)^{(NK-1)}\right] \tag{3}$$

where

$$T_{CF}(I_{be1}) = \frac{1}{T}\left(\frac{XTI}{N} - \frac{V_{BE}}{NF \cdot V_T} + \frac{EG}{N \cdot V_T}\right) \tag{4}$$

and

$$T_{CF}(I_B) = \frac{1}{T\beta_F I_B}\left[I_{be1}\left(XTI - XTB + \frac{EG - V_{BE}/NF}{V_T}\right)\right.$$
$$\left. + \frac{\beta_F I_{be2}}{NE}\left(XTI - NE \cdot XTB + \frac{EG - V_{BE}}{V_T}\right)\right] \tag{5}$$

where I_{be1} is the forward diffusion current and I_{be2} is the non-idea base-emitter current. These expressions are valid throughout the forward-active region. The new power dissipation and local temperature are then computed using the new terminal currents.

To form the thermally modified admittance matrix, the SPICE hybrid-π parameters are first converted to g-parameters. The DC equivalent of (2) is then used to compute the thermally modified g-parameters, which are converted back to hybrid-π form and loaded into the matrix.

DC convergence is checked by comparing the currents at the beginning of each iteration to those at the end. During DC sweeps, the initial current estimate at a sweep point is linearly extrapolated from the previous point. This can cause premature convergence, because the extrapolation does not reflect possible temperature changes. To avoid this, the linear extrapolation is skipped for the first iteration at each point.

4 AC Analysis

Depending on the model level specified, Z_{TH} is computed from either the supplied R_{TH} and C_{TH} or from (1). In the AC analysis the hybrid-π parameters are converted into y-parameters using

$$Y_{11e} = g_\pi + g_\mu + j\omega(C_{xcb} + C_{be} + C_{bc}) \tag{6}$$

$$Y_{12e} = -g_\mu + j\omega(C_{xcb} + C_{bc}) \tag{7}$$

$$Y_{21e} = g_m - g_\mu + j(xgm - \omega C_{bc}) \tag{8}$$

$$Y_{22e} = g_o + g_\mu + j\omega \cdot C_{bc} \tag{9}$$

where C_{be} and C_{bc} are the base-emitter and base-collector capacitances respectively, xgm is the excess phase term, C_{xcb} is a base-emitter transcapacitor controlled by the base-collector voltage, and the other terms are standard hybrid-π parameters. The thermally corrected y-parameters are then computed using (2) and loaded into the admittance matrix.

5 Simulation Results

To demonstrate the improved accuracy afforded by the thermally enhanced BJT model, a series of simulations are compared to measurements in Figs. 1-4. The device had emitter length and width of 23 μm and C-B junction depth of 3.0 μm. The fully predictive model was used, with $N_{EPI} = 10^{15}$ cm^{-3}.

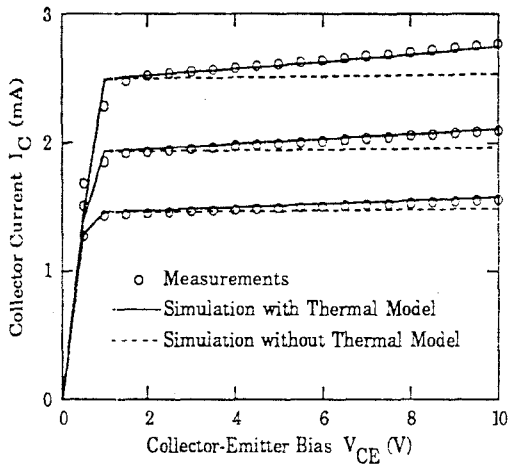

Fig. 1. Typical measured and simulated output characteristics.

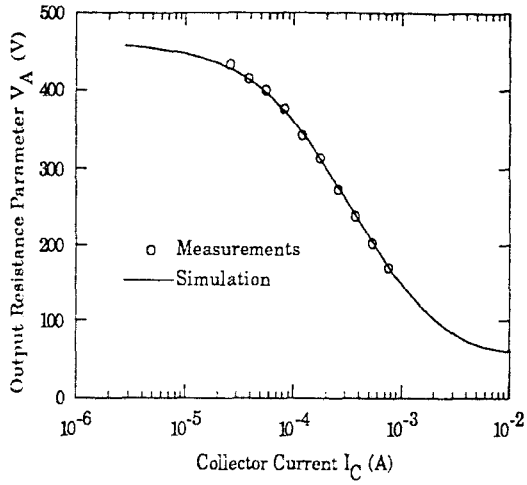

Fig. 2. Normalized output resistance $V_A=I_C/g_{22}$-V_{CE} for V_{CE}=6V. Note: Gummel-Poon model predicts a constant for this parameter.

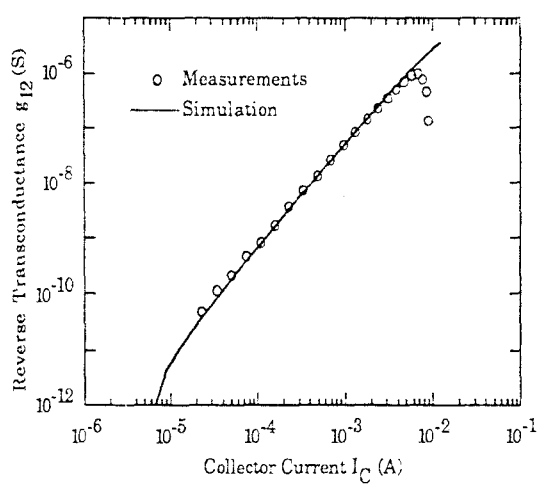

Fig. 3. Common-emitter reverse transconductance. Unmodified SPICE gives zero value for this parameter.

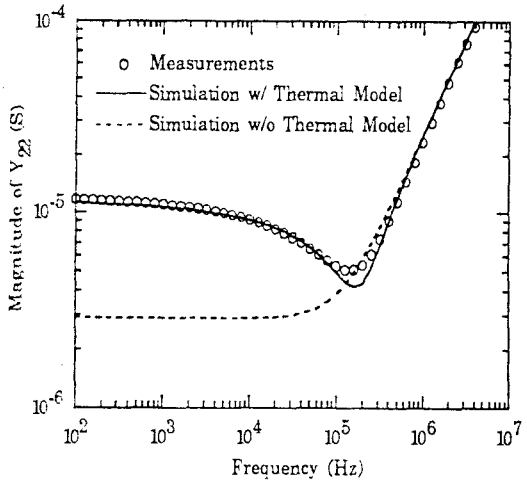

Fig. 4 Output admittance magnitude (V_{CE}=6V; I_C=1.5mA).

6 Acknowledgment

This work was supported by Semiconductor Research Corporation, Contract #91-SP-087.

References

[1] W. F. Davis and M. L. Lidke, "The effect of thermal feedback within the bipolar transistor on Gummel-Poon model accuracy," *Motorola Internal Report*, May 27, 1988.

[2] K. Fukahori and P. R. Gray, "Computer simulation of integrated circuits in the presence of electrothermal interaction," *IEEE J. Sol. St. Circuits*, vol. SC-11, pp. 834-846, December 1976.

[3] F. Q. Ye, "A BJT model with self heating for WATAND computer simulation," *IEEE Circuits and Devices Mag.*, vol. 7, pp. 7-9, 1991.

[4] R. Vogelsong & C. Brzezinski, "Simulation of thermal effects in electrical systems," APEC '89, Baltimore, MD, 1989.

[5] R. M. Fox and S.-G. Lee, "Scalable small-signal model for BJT self-heating," *IEEE Electr. Dev. Lett.*, vol. 12, December 1991.

[6] O. Mueller, "Internal thermal feedback in four-poles especially in transistors," *IEEE Proc.*, pp. 924-930, August 1964.